RB 34

DISCHARGE MECHANISM OF MERCURY POOL ARCS

RADIO CORPORATION OF AMERICA
RCA LABORATORIES
INDUSTRY SERVICE LABORATORY

RADIO CORPORATION OF AMERICA

RCA LABORATORIES

INDUSTRY SERVICE LABORATORY

RB-34

Discharge Mechanism of Mercury Pool Arcs

This report is the property of the Radio Corporation of America and is loaned for confidential use with the understanding that it will not be published in any manner, in whole or in part. The statements and data included herein are based upon information and measurements which we believe accurate and reliable. No responsibility is assumed for the application or interpretation of such statements or data or for any infringement of patent or other rights of third parties which may result from the use of circuits, systems and processes described or referred to herein or in any previous reports or bulletins or in any written or oral discussions supplementary thereto.

Discharge Mechanism of Mercury Pool Arcs

A model for the discharge mechanism of mercury pool arcs is proposed and shown to be in agreement with experiment. The conclusions drawn from this model are the following: (1) Mercury pool arcs operate in the ball-of-fire mode of discharge. (2) The electron emission mechanism is nonthermionic. Emitted electrons from the cathode arrive with only thermal energies in a plasma adjacent to the cathode. The potential of this plasma is equal to or slightly higher than that of the Fermi level of the cathode. The emission may be either due to a large electric field at the cathode surface (tunnel effect) or due to an effective lowering of the cathode work function. This lowering of the work function may be caused by a vapor or plasma of high density adjacent to the cathode surface.

I. Introduction

An arc is usually defined as a self-sustained gas discharge having a potential drop between the cathode and the anode of the order of the ionization potential of the gas or vapor in which the discharge takes place. Depending on the electron emission mechanism one can distinguish between thermionic arcs and low boiling point metal arcs. The details of the emission mechanism of the latter type of arcs are not well understood. The distinction between the two types of arcs cannot be drawn too sharply. However, it is generally believed that the electron emission in the mercury pool arc is essentially nonthermionic. The work described in this bulletin is primarily concerned with the low pressure mercury pool arc; however the basic ideas and results may also be applicable to other low boiling point metal arcs.

In 1954 it was discovered[1] that the glow region of the ball-of-fire mode of externally heated hot cathode discharges[2] exhibits retrograde motion when subjected to a transverse magnetic field just as does the cathode spot on a mercury pool cathode. The functional dependence of velocity of motion on gas pressure, current and magnetic field was found to be quite similar for the two phenomena. Based on this analogy a model for discharge mechanism of the mercury pool arc is first proposed. Conclusions drawn from this model are shown to be in agreement with experiment. These include measurements of minimum arc drop, potential and current density distributions, studies of arc motion, and pulse measurements. Studies of discharge behaviour after arc-extinguishing are shown to indicate that the electron to ion current ratio of the arc is not less than about 50. Possible electron emission mechanisms are discussed. A comparison between the power consumption for the mercury pool arc and that of thermionic arcs is made.

* This research was supported by the United States Air Force through the Air Force Office of Scientific Research of the Air Research and Development Command.

II. Model for The Discharge Mechanism of The Mercury Pool Arc

In this section a model for the discharge mechanism of the mercury pool arc will be proposed. This model is based on the following two basic assumptions: (1) Electron emission from the cathode occurs directly into a dark plasma adjacent to the cathode surface at approximately the same potential as the Fermi level of the cathode. (2) Mercury pool arcs operate in a discharge mode very similar to the ball-of-fire mode of externally heated hot-cathode discharges[2].

The essential features of the discharge model are illustrated in Fig. 1, showing cross-section of tube structure and potential distributions for a tube having short cathode to anode spacing and operating at a low current level. The potential distribution diagrams are drawn with the Fermi level of the cathode as reference point. According to this model, electron emission occurs directly into a dark (that is relatively less bright) plasma

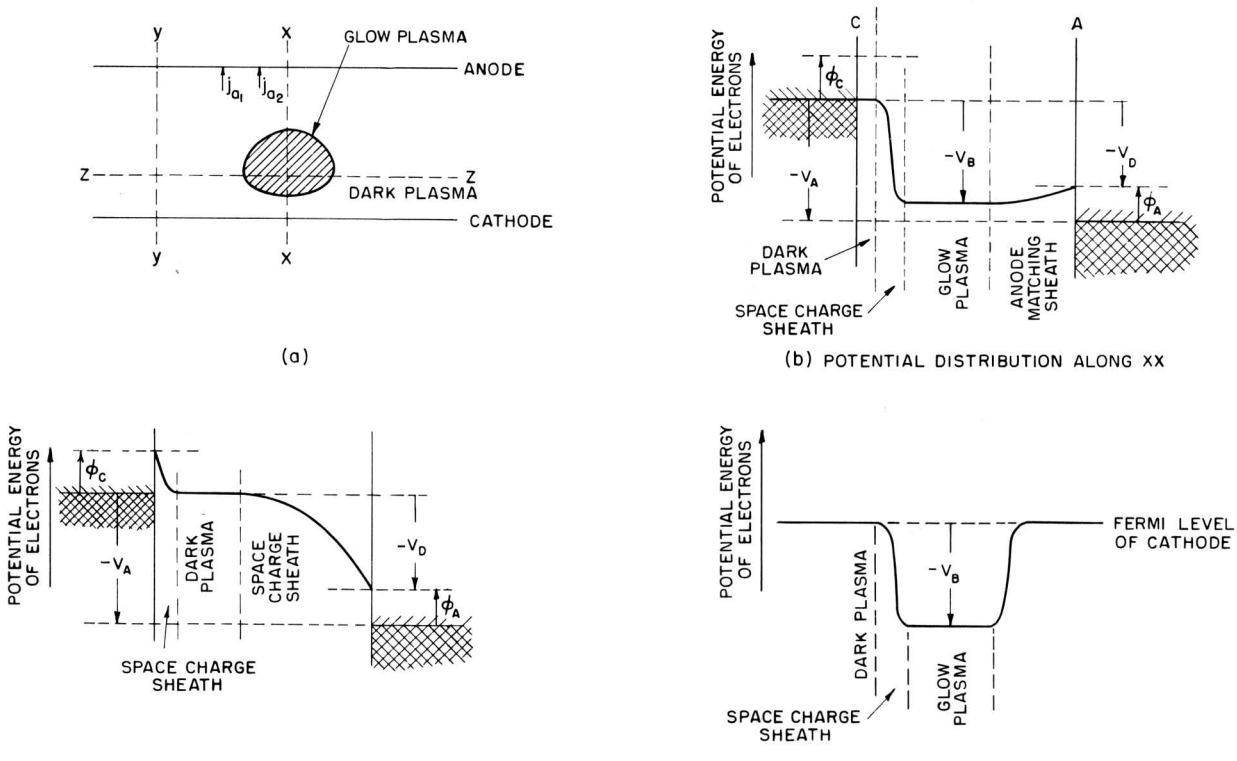

Fig. 1. Schematic diagrams showing tube structure and potential distribution for a mercury pool arc.

surrounding the glow region. It will be assumed that the electrons arrive in the dark plasma with only thermal energies either as a consequence of barrier penetration or an effective lowering of the barrier between the cathode and the plasma. The actual potential distribution within the dark plasma adjacent to the cathode surface will be further discussed in Section XIII. Adjacent to the glow plasma the potential of the dark plasma is equal to or somewhat larger than the Fermi level of the cathode. Electrons flow from the dark plasma partly directly to the anode and partly through the glow plasma. The dark plasma and the glow plasma are connected by a Langmuir double sheath such as to give essentially zero electric field at opposite edges of the sheath, except possibly at the dark plasma near the cathode. All ionization takes place in the glow plasma. Ions flow from the glow plasma into the dark plasma to supply its ion losses. The potential difference between the two plasmas, V_B, may be in the vicinity of the ionization potential of the gas or vapor in which the discharge takes place. The potential V_B, however, does not necessarily have to be as large as the ionization potential since ionization in the glow region is adequately accounted for by cumulative ionization and by energetic electrons in the tail of the Maxwellian energy distribution, provided the electron temperature is high enough. If the plasma electron space current at the anode edge of the glow region is larger than the anode current called for by the external circuit a matching sheath with a retarding field for electrons, $V_B - V_D$, will form at the anode.

To evaluate plasma potential, temperature, and size, the same procedure could, in principle, be used for the mercury pool arc as for the ball-of-fire mode of externally heated hot-cathode discharges[2]. However, because of the complicated geometry and pressure conditions of the mercury pool tube this will prove more difficult. Thus, as far as these parameters are concerned, only qualitative comparison can be made between theory and experiment. Electron temperatures in the glow plasma in the range 10000-15000 degrees K have been observed both for the mercury pool arc[3] and the ball-of-fire mode of discharge[2]. For the ball-of-fire mode, theory and experiment indicate that the size of the glow plasma decreases with pressure. Further, it has been shown that if the cathode to anode distance is increased a second glow-plasma at a higher potential will form near the anode. In the low pressure mercury pool arc the pressure is quite non-uniform, being quite high near the cathode spot and equal to the vapor pressure determined by the wall temperature far away from the cathode. Thus, theory predicts that the glow-plasma near the cathode surface should be very small in size compared to the second glow region formed at the anode. Such behavior is commonly observed in mercury pool tubes. In Fig. 2 such a case is illustrated.

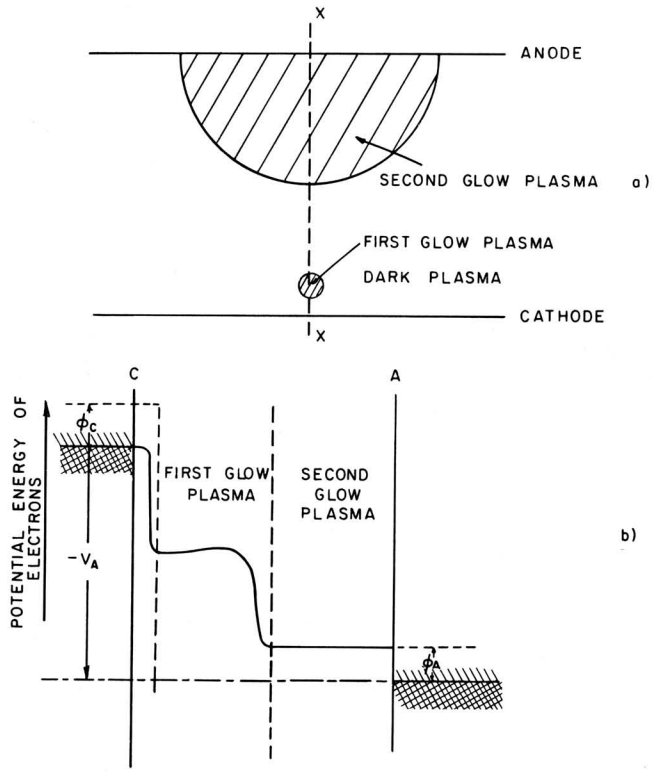

Fig. 2. Schematic diagrams showing cross-section of tube structure and potential distribution along xx for a discharge mode having two glow plasmas.

III. Potential Distributions

Measurements of the potential distribution of the mercury pool arc have been made by Kömmick.[3] The longitudinal potential distribution shown in Fig. 2(b) is consistent with Kömmick's measurements. Such a potential distribution has also been observed in the ball of fire mode of discharge by varying the cathode to anode distance[2]. Kömmick did not measure the transverse potential distribution close to the cathode where the small first-glow region is situated.

In Fig. 3 (a) tube structure and circuit that was used for studying the transverse potential distribution is shown. The tube was a continuously pumped diode with a ring-shaped mercury pool cathode C and a soft iron anode A, toroidal in form but with wedge shaped cross-section. The average circumference of the anode was 89 millimeters and the anode-to-cathode distance was about 1/2 millimeter. For studies of the potential distribution of the arc, a tungsten wire W of 0.003 inch diameter was supported between the cathode and the anode. The anode was grounded and the cathode was connected through a limiting variable resistor R to a 110 volt d-c power supply. The probe wire, W, was connected directly to an oscilloscope. The tube was placed in the gap of an electromagnet with an annular structure giving a radial magnetic field as shown in Fig. 3.

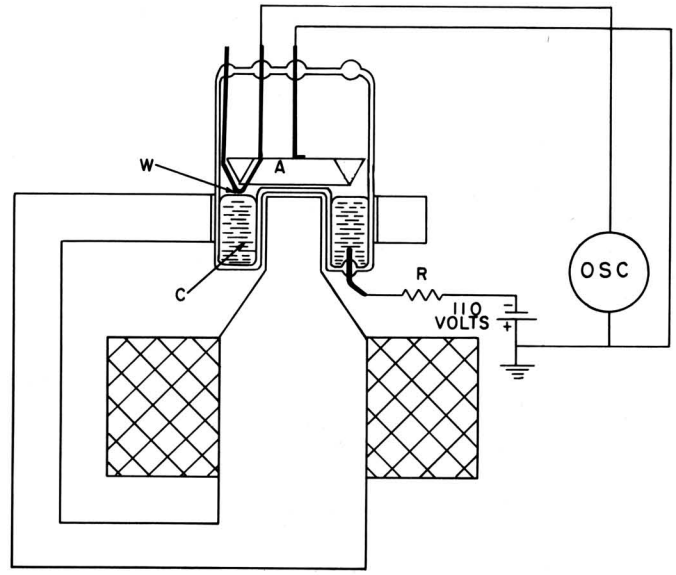

Fig. 3. Schematic drawing of tube and circuit for studying potential distribution of the mercury pool arc.

When started, the arc races around continuously in a circular path, the direction of motion being of course, retrograde. As the arc passes by the probe the potential between the probe and the anode is recorded. In Fig. 4 a typical oscillogram is shown. The light output from the arc was monitored and was shown to coincide with the sharp peak of Fig. 4. This, then, may be identified with the glow region. It is seen that the potential distribution recorded by the probe agrees qualitatively with that predicted by the discharge model, shown in Fig. 1 (d). This method does not allow a quantitative evaluation of the plasma potential since the actual plasma electron temperatures in both plasmas are not known. Furthermore, due to the fact the probe had a finite extension, different parts of the probe may have been located in parts of the plasma at different potentials. The probe may thus have greatly disturbed the actual behaviour of the arc.

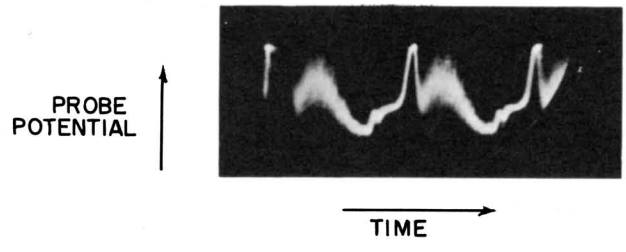

Fig. 4. Oscillogram of probe potential.

IV. Arc Energy Balance

In accordance with the discharge model proposed above, the voltage drop V_D available for the discharge is, referring to Fig. 1.,

$$V_D = V_A - \phi_A . \tag{1}$$

Here, V_A is the actual anode voltage as measured between the cathode and anode lead and ϕ_A is the work function of the anode. Neglecting the losses due to recombination and elastic impacts with neutral atoms, the major losses of energy in the arc are:

(1) For generating excited atoms P_{ex}.

(2) For generating ions $V_i I_p$, where V_i is the ionization potential and I_p is the ion current flowing to the cathode.

(3) Energy picked up by ions $(V_B + \phi_c) I_p$, where ϕ_c is the work function of the cathode.

(4) Energy carried into the anode by the energetic electrons[4] leaving the glow region $2 I_e \frac{kT_e}{e}$, where I_e is the electron current flowing to the anode and T_e is the electron temperature of glow region.

Here the ion current flowing to the anode has been neglected. Assuming that the major part of the electron current flows through the glow plasma and that the energy carried by the ions to the cathode $(V_i + V_B) I_p$ is consumed in evaporating cathode material, one obtains, equating energy input to energy sinks,

$$V_D I_A = P_{ex} + V_i I_p + (V_B + \phi_c) I_p + 2 I_e \frac{kT_e}{e} \tag{2}$$

Here, the anode current $I_A = I_e + I_p$, k is the Boltzman constant, and e the electronic charge. As is shown in Section VII-2, $I_e/I_p \cong 50$. Thus equations (1) and (2) can be written as:

$$V_A \cong \phi_A + \frac{P_{ex}}{I_A} + \frac{I_p}{I_e} (V_i + V_B + \phi_c) + 2 \frac{kT_e}{e} \tag{3}$$

Equation (3) then gives the minimum possible anode voltage for maintaining the arc. The most difficult term to estimate in this equation is P_{ex}/I_e. However, measurements of the total radiation output using a thermopile has shown that P_{ex}/I_e lies between 0.1 and 0.5 volts. The term $I_p/I_e (V_i + V_B + \phi_c)$ is of the order of 0.5 volts. For ordinary cathode materials, ϕ_A lies between 4 and 5 volts. As mentioned in Section II, T_e lies between 10000 and 15000 degrees K, corresponding to a value of $2\frac{kT_e}{e}$ between 2 and 3 volts. Thus the minimum anode voltage V_A may be expected to lie between 6.6 and 9 volts. This is in good agreement with the value of 7.3 volts reported in the literature.[5]

It is interesting to note that the voltage V_D available for the discharge is 2.6 to 4 volts. To attain such a low arc drop one would have to use a low work function anode material. Unfortunately, such anode materials are not suitable in mercury pool tubes.

V. Current Density Distribution

In order to assure sheath stability it is necessary that the glow region and the dark plasma be joined by a Langmuir double sheath which makes the electric field at opposite edges of the sheath essentially zero. This criterion for sheath stability, which determines the ratio of plasma density of the glow region N_2 to that of the dark plasma N_1, can be expressed as[1]

$$\frac{j_p}{j_e} = \frac{N_2 v_{p2}}{N_1 v_{e1}} = \sqrt{\frac{m_e}{m_p}} . \tag{4}$$

Here, j_p and j_e are the ion and electron current densities respectively, v_{p2} is the average velocity of ions entering the sheath from the glow region, and v_{e1} is the average velocity of electrons entering the sheath from the dark plasma. The quantities m_e and m_p are the electron and ion masses respectively. If T_{p2} is the ion temperature of the glow region and T_{e1} is the electron temperature of the dark plasma, equation (4) can be written as

$$\frac{N_2}{N_1} = \frac{v_{e1}}{v_{p2}} \sqrt{\frac{m_e}{m_p}} = \sqrt{\frac{T_{e1}}{m_e}} \sqrt{\frac{m_p}{T_{p2}}} \sqrt{\frac{m_e}{m_p}} ,$$

or

$$\frac{N_2}{N_1} = \sqrt{\frac{T_{e1}}{T_{p2}}} , \tag{5}$$

The anode current density j_{a2} beyond the glow region (see Fig. 1) is

$$j_{a2} = eN_2 v_{e2} e^{-\frac{(V_B - V_D)e}{kT_{e2}}} , \tag{6}$$

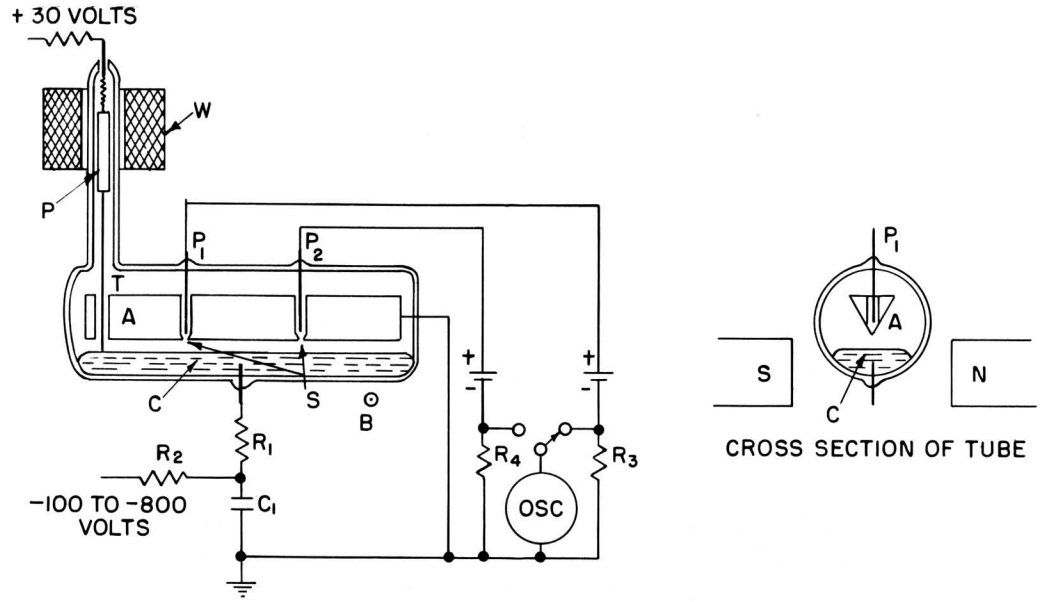

Fig. 5. Schematic drawing of tube and circuit for studying current distribution of mercury pool arc.

where v_{e2} is the average velocity* of electrons entering the anode sheath and T_{e2} is the electron temperature of the glow region. The anode current density j_{a1} beyond the dark plasma (close to the glow region) is

$$j_{a1} = eN_2 v_{e1} . \tag{7}$$

From (5), (6), and (7)

$$\frac{j_{a2}}{j_{a1}} = \frac{N_2}{N_1}\,\frac{v_{e2}}{v_{e1}} = \sqrt{\frac{T_{e1}}{T_{p2}}}\sqrt{\frac{T_{e2}}{T_{e1}}}\; e^{-\frac{(V_B - V_D)e}{k\,T_{e2}}}$$

$$\frac{j_{a2}}{j_{a1}} = \sqrt{\frac{T_{e2}}{T_{p1}}}\; e^{-\frac{(V_B - V_D)e}{k\,T_{e2}}} \tag{8}$$

Assuming $T_{e2} \approx 10000 - 15000^{\circ}K$, $T_{p2} = 300^{\circ}K$, and $V_B \approx V_D$, one obtains $j_{a2}/j_{a1} \approx 4\text{-}5$. Thus, in this case, the anode current density beyond the glow region may be expected to be 4 to 5 times that beyond the dark plasma.

In order to study the arc current density distribution a tube structure similar to one employed by Smith[6] was used. Fig. 5 shows the tube and circuit. The tube was a continuously pumped diode with a mercury pool cathode C and a wedge-shaped soft iron anode A. The anode was 2 1/2 inches long and the cathode to anode distance was about 1/2 millimeter. In the anode were cut two 0.002 inch wide slits, S. Behind the slits were placed electrodes P_1 and P_2. An arc was started at one end of the tube by a method in which a current carrying wire T, in contact with the mercury pool, was suddenly pulled up by means of the plunger P and coil W. The anode was grounded and the cathode was connected to ground through a current limiting resistor and a large capacitor C_1. C_1 was charged up negatively by a power supply through a large resistor R_2. The electrodes P_1 and P_2 were biased slightly positive with respect to ground and the currents to these electrodes were monitored by an oscilloscope connected across the small resistor R_3 and R_4. A transverse magnetic field was applied by means of an electromagnet.

When started, the arc was immediately taken up by the main anode A and raced, as a result of the transverse magnetic field, in the retrograde direction along the anode to the opposite end of the tube. When the capacitor C_1 was discharged the arc extinguished. After the capacitor C_1 had again charged up the process could be repeated. The currents to P_1 and P_2 were observed and oscillograms photographed as the arc raced by the slits, S. Fig. 6 shows typical oscillograms for different magnetic fields B. In Fig. 6 the anode current I_A is shown on the same time scale.

From Fig. 6 it is seen that as the arc approached the slit, the current at first increased quite slowly, then increased sharply to a 4 to 5 times higher value. Similarly at the trailing edge of the arc, the current first drop-

*The average velocity of electrons entering the sheath is $\bar{c}/4$, where $\bar{c}$ is the average Maxwellian velocity.

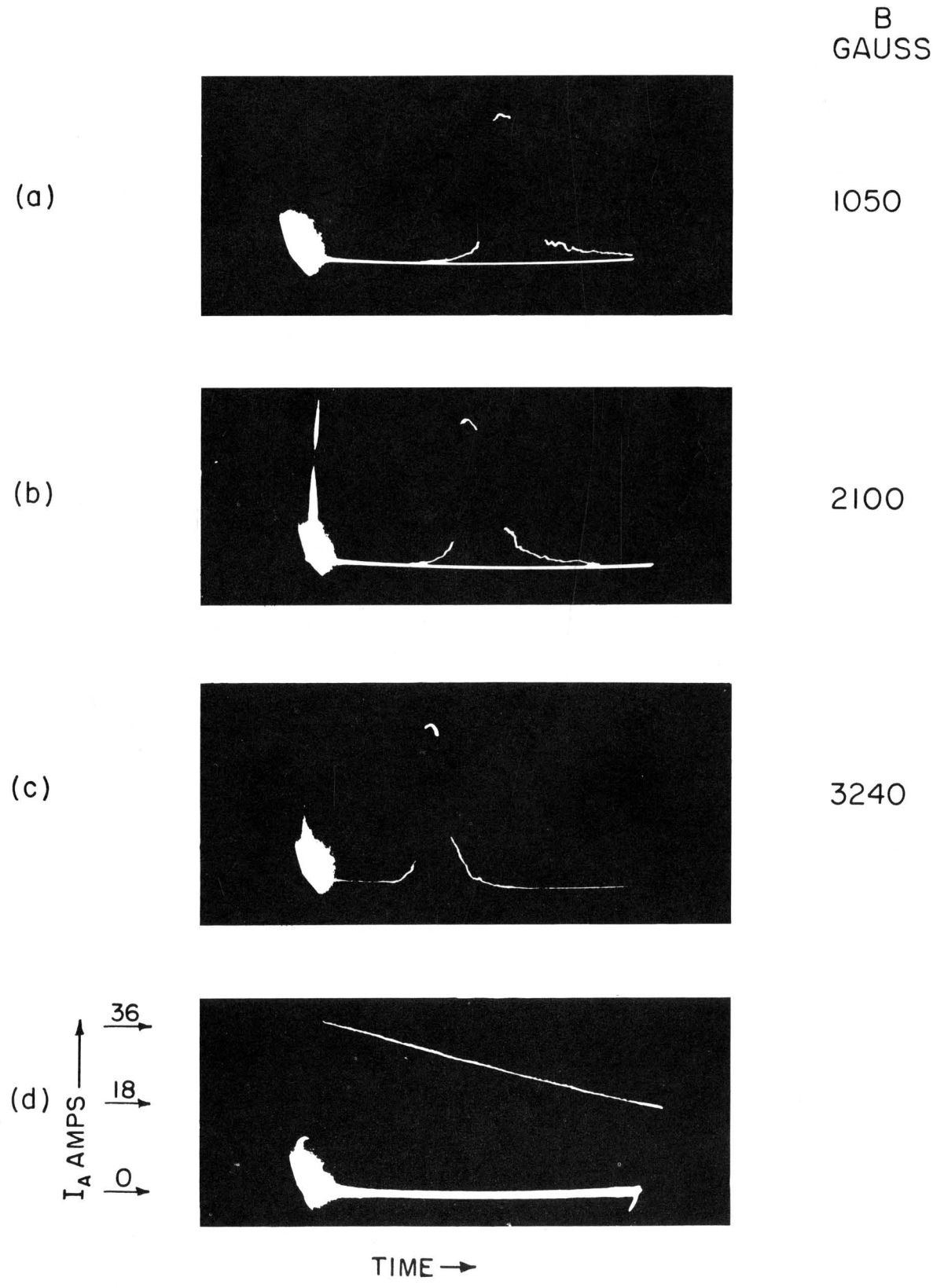

Fig. 6. Oscillograms of current to electrode P_1 for different values of magnetic field B (a-c). Oscillograms of anode current I_A on same time scale (d).

ped sharply and then decayed slowly. This behavior is in agreement with that predicted by the discharge model.

By measuring the time displacement of the signals to P_1 and P_2 the spot velocity was found to be 3.5 meters/sec at 2670 gauss. The actual length of the glow region was 6.6 mm.

VI. Motion of Arc Cathode Spot

The motion of the arc cathode spot over the cathode surface is intimitely connected with the stability criterion for the space charge sheath connecting the two plasmas as expressed by equation (4). Because of the high electron temperature and the anomalously high scattering[1,2] of electrons in the glow plasma this region is much less subject to density disturbances than the dark plasma. Thus, in these discussions, the glow plasma can, to a first approximation, be considered as a stable entity as far as size, electron temperature, and plasma density are concerned. The dark plasma on the contrary is quite easily subject to density disturbances. In general, the glow plasma will adjust itself to such a position as to make the ion-losses of the dark plasma equal on both sides of the glow plasma. A natural stable position may be one in which the glow plasma is symmetrically located in the depression[5] caused by the discharge itself on a free mercury surface as shown in Fig. 7(a). Due to wave motions set up on the mercury surface, the glow plasma can be expected to ride along in the trough of a wave and thus move erratically over the mercury surface. Also, a non-symmetrical depression in the mercury surface may give a net horizontal component of arc pressure on the surface, making the velocity of motion current-dependent[7]. Another stable position for the glow region would be at the wetting line of an electrode protruding out of the mercury surface[5], as shown in Fig. 7(b). This may be the explanation for the anchoring of the cathode spot at such a wetted electrode. Finally, a third stable position for the glow region would be in a groove cut in a solid cathode wetted with mercury. This has been found to be the case[8] in an experiment where a groove was cut in a wetted metal stump protruding out of the mercury, the groove being above the junction line between the metal stump and the mercury.

Of particular interest are disturbances caused by an external magnetic field perpendicular to the current flow between the cathode and the anode. This kind of disturbance leads to the well known phenomenon of retrograde motion[9,10] wherein the glow region of the arc moves in a direction opposite to the electromagnetic force on the moving charges. Assume that the density distribution for the undisturbed arc is such as to satisfy equation (4) along the boundary between the dark plasma and the glow plasma. To a first approximation the effect of an applied transverse magnetic field will be to bend the electron flow through the cathode region in the direction of the electromagnetic force. The density of the dark plasma will then be increased on one side of the glow region and decreased on the other side. This will lead to violation of the criterion for sheath stability (equation 4). Just as for the case of the ball of fire mode of hot cathode discharge[1], sheath stability can again be restored if the glow region moves through the gas in the retrograde direction at a velocity given by

$$v_B = 36.4\,\mu^- GB \sqrt{\frac{T_{p2}}{M}} \text{ meters/second.} \qquad (9)$$

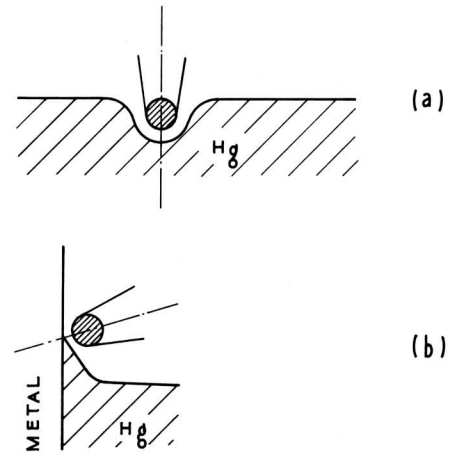

Fig. 7. Diagrams showing stable position of symmetrically adjusted glow region (a) in the trough of depression in a free mercury surface and (b) at the wetting line of an electrode protruding from the mercury surface.

Here μ^- is the electron mobility of the dark plasma, B the magnetic field in Gauss, and M the molecular weight of the ions. G is a geometrical factor which can only be determined from a complete solution of the flow conditions in the dark plasma. Essential for this mechanism of retrograde motion is that the electrons when traveling from the cathode surface to the space charge sheath surrounding the glow plasma exhibit a plasma like behavior. That is to say, their motion is one of drift by virtue of density gradients and weak electric fields.

The behavior described above is corroborated by the oscillograms shown in Fig. 6. It is seen that the current through the dark plasma is somewhat lower at the leading edge than at the trailing edge of the glow region. Further, this dissymmetry is seen to increase with mag-

netic field. (This dissymmetry is somewhat larger than seen in the oscillograms because the anode current actually decreases during the passage of the arc past the slit, as seen in Fig. 6(d).) This behavior is identical to that in the ball of fire mode of hot cathode discharges[1].

Equation (9) is true only for relatively small disturbances (low magnetic fields). At higher velocities a saturation effect of the velocity is usually observed.[9,10] This may be due to the apparent change in the mobility and diffusion constants caused by the magnetic field and also due to the neglected change in the flow conditions of the glow region. It appears that an expression of the form

$$v_B = 36.4\, G\, \frac{\mu^- B}{1 + (\mu^- B)^2} \sqrt{\frac{T_{p2}}{M}} \qquad (10)$$

fits the data obtained by St. John and Winans[9] quite well for a value of $\mu^- = 1.25 \times 10^4$ cm^2/voltsec. Since a complete solution of the plasma flow equations has not been obtained even for small disturbances it is not obvious that such an expression should be valid. However, the expectation value[11] of the transverse displacement of the electron flow through the dark plasma in the presence of a weak electric field depends on the magnetic field in exactly the same manner as does v_B according to equation (10). For a value[12] of $\mu^- = 5.2 \times 10^5$ cm^2/voltsec at a pressure of 1 mm of mercury and a temperature of 273 degrees K, the above value of $\mu^- = 1.25 \times 10^4$ cm^2/voltsec yields a value of the average pressure equal to 22 mm of mercury for an electron temperature of 1000 degrees K. As will be shown later in section VII, a value of the same order of magnitude is obtained for the pressure in the glow region.

A further discrepancy from equation (9) is usually observed for the velocity of motion. At a specific velocity, which is about 10 meter/sec. for a glow region moving over a free mercury surface[10] and about 100 meter/sec for a glow region moving along a meniscus[9], a sudden fast rise in velocity occurs with increasing magnetic field. For a glow region moving in a groove cut in a solid cathode wetted with mercury this effect is not observed[8]. This suggests the following explanation for the sudden increase in velocity: at relatively low speed the glow region will be located in the depression in the mercury surface caused by the arc itself, as shown in Fig. 7(a). Even for an anchored arc there will be a depression in the level of the meniscus. This geometry condition of the glow region in the depression corresponds to a specific value of the geometrical factor G in equations (9) and (10). As the speed is increased a critical speed is finally reached at which the inertia effect of the mercury becomes so great that the depression of the mercury surface becomes increasingly less deep. As the glow region raises out of the mercury the factor G changes. It is reasonable to assume that it will increase because the critical side boundaries of the glow region move away from the mercury surface. As G increases a still larger velocity v_B is called for according to (9) and (10). Thus a fast increase in velocity will occur until the glow region moves completely above the mercury surface, as shown in Fig. 1(a). From this point on, the v_B versus B relation may again be given by an expression such as (10), however with a larger value of the geometrical factor G. This behaviour is in agreement with experiment. It shows that this sudden velocity-increase should not be observed for a glow region moving in a groove cut in a solid cathode wetted by mercury and also why in this case, because of the larger value of G, the observed velocity[8] is larger even at low values of B.

VII. Transient Behavior of The Mercury Pool Arc

It was found by Mierdel[13], and verified by Engelbrecht[14], that the arc will extinguish if the anode current is instantly brought down to zero from its running d-c value, for times as short as 10^{-9} seconds. No measurements were made of the actual anode voltage at which extinguishing occurred nor was the discharge behavior immediately after arc-extinguishing studied. In this section will be described an experiment using pulse techniques for further studies of these effects.

Pulse Measurements on the Mercury Pool Arc

The tube used in these tests was a continuously pumped diode, having a mercury pool cathode and a molybdenum anode. The cathode-to-anode spacing was about 1/2 inch. The arc spot was anchored at a wetted molybdenum surface protruding from the mercury surface.

The circuit used is illustrated schematically in Fig. 8. The tube was connected in series with a current limiting resistor R_L and a small resistor R_I to the power supply (110 volt d-c line voltage in parallel with a large condensor). The anode voltage V_a and current I_a were monitored by oscilloscopes. Also, the light output from the tube was monitored by means of a 929 photo tube and oscilloscope. The pulser was so devised that it instantly brought down the anode voltage and current from the running d-c arc values, V_{ao} and I_{ao}, to lower values, V_{aD}, and I_{aD} for the duration of the pulse.

Typical oscillograms are sketched in Fig. 9, where anode voltage and current are plotted against time. By measuring the value of anode voltage V_{aD} and anode cur-

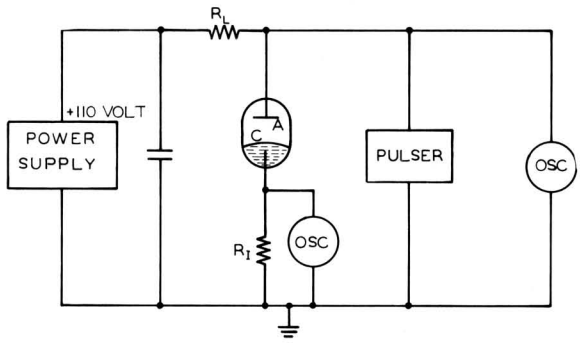

Fig. 8. Schematic diagram of circuit for pulse measurements on the mercury pool arc.

rent I_{aD} during the application of the pulse, "dynamic" volt-ampere characteristics can be plotted for different pulse lengths. Also by noticing the values for which the arc extinguishes, the necessary "keep-alive" power can be calculated.

The result of such measurements is shown in Fig. 10 together with the d-c characteristic of the arc, marked DC. In the range 25 to 200 microseconds the arc impedance varies greatly during the application of the pulse. In this case neither the voltage nor the current pulse were square and V_{aD} and I_{aD} were measured at the end of the pulse. Oscillograms of the monitored light output for the points close to arc extinguishing showed that for pulse lengths of the order of a microsecond the plasma decay is negligible. Thus the discharge acts as if the plasma density were "over-saturated". According to equation (6), this requires a larger retarding field for electrons at the anode space charge sheath than d-c conditions for the same anode current. It was found that the current can be pulsed down to almost zero without extinguishing of the arc. Thus, only a very low keep-alive power is required. However, when the current approaches the value zero, arc-extinguishing occurs. At pulse lengths of the order of 10 microseconds significant plasma decay and diffusion occurs, resulting in a rapid change of arc impedance with time. Also, the keep-alive power increases. At 200 microseconds the arc has re-established itself to new equilibrium conditions essentially equivalent to those of the d-c arc. Thus, there appears to exist two criteria for keep-alive of the arc: (1) the arc current must be larger than zero but may be as low as 10 to 100 milliamperes: (2) the glow plasma must not decay below a certain critical density.

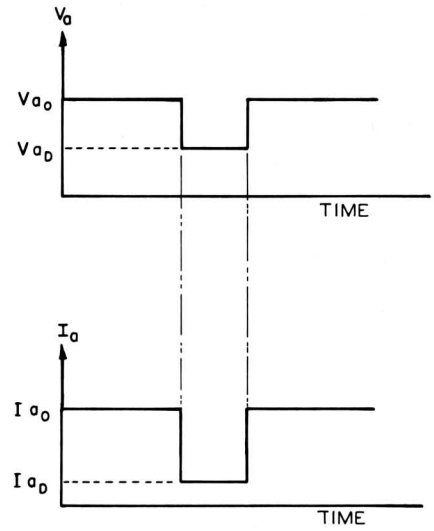

Fig. 9. Typical pulse shapes showing anode voltage (above) and anode current (below).

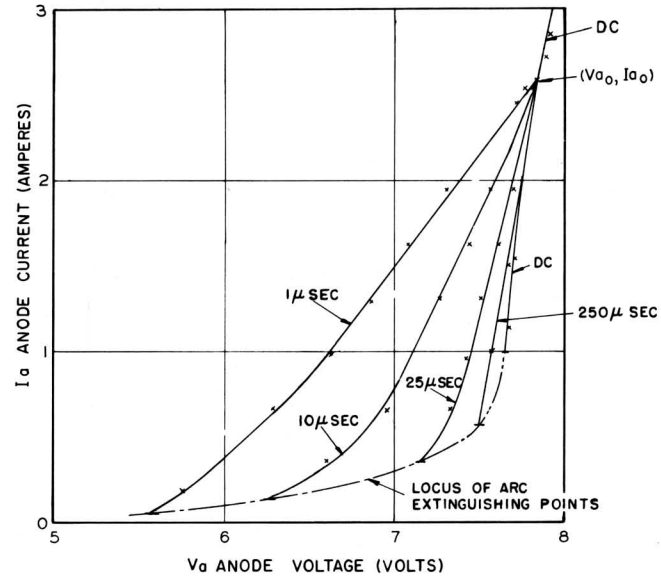

Fig. 10. Dynamic volt-ampere characteristics with pulse length as parameter.

Of particular interest, is the fact that for short current interruptions the anode current approaches zero for an anode voltage between 5 and 6 volts which is slightly higher than the work function of the anode (4.3 volts). This behavior is significantly different from that of a thermionic arc. A similar experiment carried out on a carbon arc in air indicated that the anode current approached zero only when the anode voltage approached zero. This indicates that for the mercury pool arc electrons emitted from the cathode came from the top of the Fermi energy distribution in the cathode and thus well below the top of the potential barrier at the surface. This is in agreement with the discharge model proposed in Section II.

Studies of Discharge Behavior After Arc Extinguishing

Since arc-extinguishing has been found to occur upon current interruptions during times as short as 10^{-9} seconds[13] it is probably safe to assume that the cathode

surface has lost its high emission capability at times of the order of a fraction of a microsecond after arc-extinguishing. The discharge behavior then should be equivalent to that of a decaying plasma left between two non-emitting electrodes. This situation is illustrated in Fig. 11 for a plane parallel structure of area A and a positive anode voltage. The plasma potential will be slightly higher by an amount V volts than the anode potential. To the cathode flows the saturated ion current en_1v_pA, where n_1 is the plasma density at the cathode edge, v_p the average velocity of ions leaving the plasma, and e is the electronic charge. To the anode flows an ion current en_2v_pA and electron current $en_2v_e e^{-eV/kT_e}A$, where n_2 is the plasma density at the anode edge, v_e is the average velocity of electrons leaving the plasma, and T_e is the electron temperature. The anode current is thus

$$I_A^+ = Ae\,(n_1v_p) = Ae\,(n_2v_e e^{-\frac{eV}{kT_e}} - n_2v_p) \qquad (11)$$

satisfying the charge neutrality requirement for the plasma

$$n_1v_p + n_2v_p = n_2v_e e^{-\frac{eV}{kT_e}} \qquad (12)$$

Thus

$$I_A^+ = Aen_1v_p \qquad (13)$$

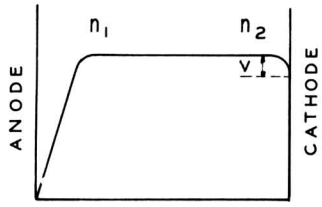

Fig. 11. Diagram showing potential distribution after arc-extinguishing for positive anode voltage.

Similarly for negative anode voltage, the anode current is

$$|I_A^-| = Aen_2v_p \qquad (14)$$

The ion current flowing to the cathode for the d-c arc is $I_p = Aen_1v_p$. Thus, immediately after arc-extinguishing, before appreciable diffusion and plasma decay has set in, the anode current for positive anode voltage is equal to the ion current flowing to the cathode for the d-c arc. If, for the d-c arc, the anode current is I_A and the electron current is I_e, one obtains from Equation (13), in case $I_e >> I_p$,

$$\frac{I_e}{I_p} \cong \frac{I_A}{I_p} = \frac{I_A}{I_A^+} . \qquad (15)$$

For studies of the discharge behavior after arc extinguishing the circuit illustrated in Fig. 12 was used.

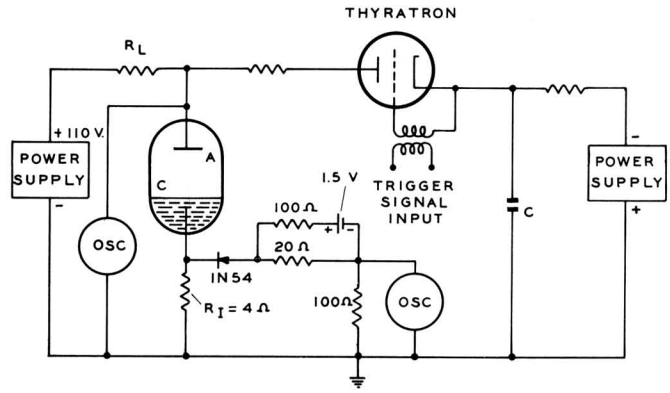

Fig. 12. Schematic diagram of circuit for studying discharge behavior after arc extinguishing.

A d-c anchored arc was operated by means of the power supply and current limiting resistor R_L. The arc was suddenly extinguished by switching, with a thyratron, a negatively charged capacitor C across the tube. Depending on the voltage to which the capacitor C was charged, the anode voltage after arc-extinguishing could be made either positive or negative. For measurements of the small discharge current flowing after arc-extinguishing, the signal picked up across the small resistor R_I was biased off by means of the crystal diode and battery as shown in the figure. In Fig. 13 is shown a d-c calibration curve for this circuit.

In Fig. 14 are shown typical oscillograms of the anode current after arc-extinguishing. These may be understood under the assumption that $n_1 > n_2$. At first there is a fast diffusion mode which establishes uniform plasma density and causes the plasma density to decrease at the cathode edge and increase at the anode edge. Thereafter, slower uniform plasma density decay takes place. In accordance with equations (13) and (14) the anode current for positive and negative anode voltage will behave as shown in Fig. 14.

An analysis of the decay curve shown in Fig. 14(a) shows that it exhibits exponential decays corresponding to time constants of $\tau_1 \cong 1.8$ microseconds and $\tau_2 \cong 100$ microseconds. Assuming that the fast decay is due to a first order diffusion mode, the characteristic diffusion length, $\Lambda = \sqrt{\tau_1 D_a}$, can be calculated. Here the ambi-

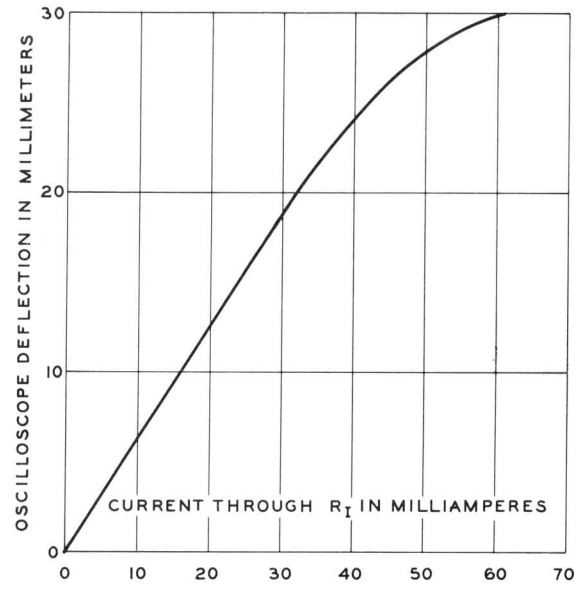

Fig. 13. DC calibration of current measuring circuit. Oscilloscope deflection is 32 millimeters at a current of 2.5 amperes through R_I.

bolar diffusion constant $D_a \cong D_p\ (1 + \frac{T_e}{T_p})$, where D_p is the diffusion constant for ions, and T_e and T_p are the electron and ion temperature respectively at a pressure of 1 mm of mercury and a temperature of 273 degrees K. For[12] D_p = 5 $cm^2/sec.$, T_e = 10,000 degrees K, T_p = 700 degrees K, and taking for Λ the value of the thickness of the glow region, 4 x 10^{-3} cm as measured by Smith[6], one obtains for the average pressure in this region a value of 12 mm of mercury. This is in reasonable agreement with the value of 22 mm of mercury obtained for the surrounding dark plasma (section VI).

From Fig. 14(a) it is seen that I_A^+ is 50 milliamperes for I_A = 2.45 amperes. Thus according to equation (14), I_e/I_p = 50 for the d-c arc. The value of I_e/I_p was found to be of the order of 50 for anode currents in the range 1 to 4 amperes. A similar value of I_e/I_p was also found for non-anchored arcs. This high value of electron to ion current for the arc indicates that the electron emission from the cathode can not be thermionic, since the energy carried by the ions to the cathode is much too low to maintain the energy balance[15] at the cathode. If the mercury pool arc were to operate as a thermionic arc, I_e/I_p would have to be less than about 5.

VIII. Discussion of the Emission Mechanism of Mercury Pool Arcs

For the discharge model proposed in Section II the following broad assumption was made concerning the

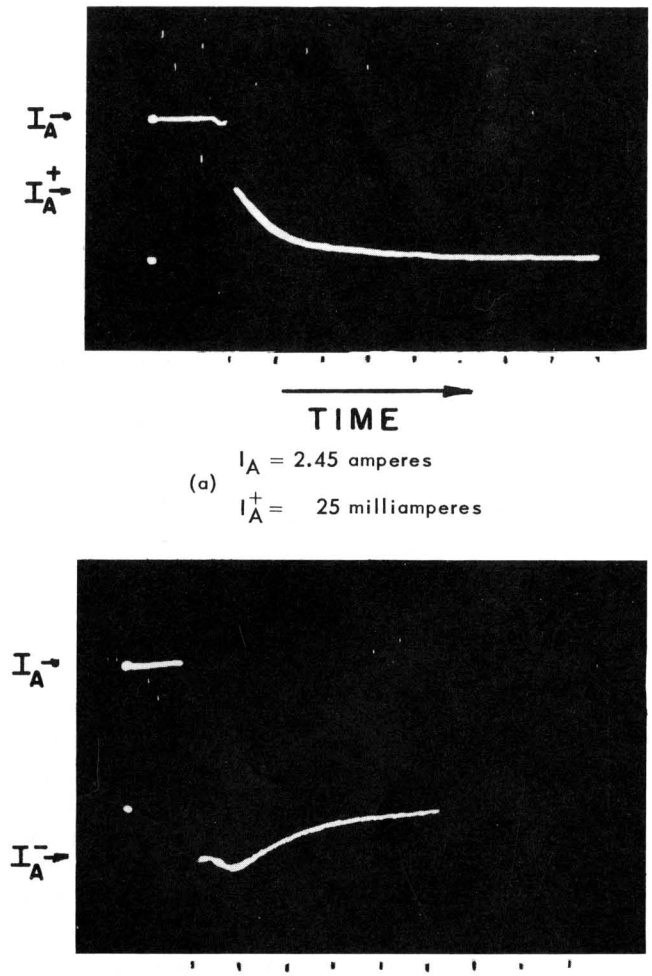

Fig. 14. Oscillograms showing anode current versus time after arc-extinguishing for positive anode voltage (a) and negative anode voltage (b). Time scale is 3 μ sec./division.

electron emission mechanism from the cathode. Electrons emitted from the cathode arrive with only thermal energies at a point outside the cathode surface which has a potential essentially equal to that of the Fermi level of the cathode*. This is equivalent to saying that electrons emitted from the cathode come from the top of the Fermi energy distribution in the cathode and not from the top of the potential barrier of the undisturbed mercury surface. This feature of the emission mechanism is in agreement

*This behavior is significantly different from the case of thermionic emission wherein the energy of the electrons at a point with the same potential outside the cathode would be larger by an amount equal to the work function of the cathode.

with the energy balance equation (section IV) and with the fact that the anode current approaches zero for an anode voltage slightly larger than the work function of the anode (section VII). The behavior is analogous to that of field emission[16] (tunnel effect) where there is a large applied electric field at the cathode. However, it is complicated by the following circumstances: (1) The large electric field at the cathode is not due to the applied field but is, instead, due to the space charge of the positive ions in the vicinity of the cathode (except for very short arcs[17] which are not considered here), (2) in the mercury pool arc there exists, almost certainly, a vapor[18] or plasma at a very high density immediately adjacent to the cathode surface. The broad assumption concerning the emission mechanism made in section II also includes the possibility of an effective lowering of the cathode work function to a very low value, say less than one volt.

Since the details of the emission mechanism are not know at present the potential distribution within the region termed "dark plasma" adjacent to the cathode surface was not specified in section II. Based on experimental evidence the properties of this region can be summarized as follows: (1) Its thickness[6] is less than 10^{-4} cm. (2) The potential within this region does not exceed that of the cathode Fermi level by more than about a volt. (3) Due to the cathode evaporation a large vapor pressure is likely to build up in this region[18]. (4) It exhibits a plasma-like behavior at least as far as the electron conduction is concerned. This is necessary for the proposed explanation for the retrograde motion. (5) This region quickly (in times of the order of 10^{-8} to 10^{-9} seconds) loses its ability to support electron conduction from the cathode if the arc current is momentarily cut to zero[13,14]. (6) The light generated in this region contains a continuous spectrum[6] in addition to the mercury line spectrum. (7) The small, intensely bright spots usually observed in mercury pool arc discharges may be due to the light generated in this region[19].

The following mechanisms of emission may be in compliance with these properties of the dark plasma. (1) Field emission due to a large electric field caused by the positive space charge adjacent to the cathode. Here the positive ions accelerated in the space charge sheath at the glow region are probably effectively slowed down in front of the cathode surface due to the high vapor pressure. The electric field at the cathode surface, then, cannot be obtained from a calculation of the space charge sheath at the glow region [20,21]. (2) Metallic conduction through a layer of very dense metallic vapor[18]. (3) Electron emission through a plasma of extremely high density[22].

Present knowledge of the region adjacent to the cathode surface is not sufficient to decide in favor of any one of these possible mechanisms of emission. Of particular importance for future work is a knowledge of the actual emission current density.

IX. Comparison Between the Mercury Pool Arc and Thermionic Arcs

An illustrative comparison can be made between different types of arcs on the basis of the arc energy balance relation. For simplicity it will be assumed that $V_B - V_D = 0$ (see Fig. 1b) and that the ion current flowing to the anode can be neglected. For the mercury pool arc the minimum anode voltage or in other words the minimum power consumption in watts per ampere is given by Equation (3), section IV.

For a thermionic arc, such as a carbon arc, the voltage drop available for the discharge is $V_D = V_A + \phi_c - \phi_A$ in accordance with Fig. 1(b). Thus the energy balance equation can be written as:

$$(V_a + \phi_c - \phi_A)\, I_A = P_{ex} + V_i I_p + I_p (V_A + \phi_c - \phi_A) + 2I_e \frac{kT_e}{e} \qquad (16)$$

Energy balance at the cathode[15] requires that

$$(V_A + \phi_c - \phi_A)\, I_A + V_i I_p - \phi_c I_p = \phi_c I_e + P_{HL} \qquad (17)$$

where P_{HL} is power lost at the cathode by heat radiation and heat conduction. Combining (16) and (17) one obtains

$$V_A = \phi_A + \frac{P_{ex}}{I_A} + 2\frac{I_e}{I_A}\frac{kT_e}{e} + \frac{P_{HL}}{I_A}. \qquad (18)$$

For a carbon arc, P_{HL}/I_A may be several watts per ampere[15] and $I_e/I_A \approx 5/6$. Also T_e may be equal to or higher than that of the mercury pool arc indicating that the latter type of arc is more efficient than the carbon arc.

For an externally heated hot cathode arc, I_p/I_e is of the order of 1/100 and for this type of arc equation (16) can be written as[2]

$$V_A = \phi_A - \phi_c + \frac{P_{ex}}{I_A} + 2\frac{kT_e}{e}. \qquad (19)$$

This equation reveals the interesting experimentally observed effect[23] that the externally heated hot cathode arc can be operated with a negative anode voltage provided ϕ_A is small (barium-covered nickel anode) and ϕ_c is large (tungsten cathode). Here, of course, the power is delivered from the heater power supply. The heater power is

$$P_H = \phi_c I_A + P_{HL} \cdot \tag{20}$$

Thus (19) can be written as:

$$V_A + \frac{P_H}{I_A} = \phi_A + \frac{P_{ex}}{I_A} + 2\,\frac{kT_e}{e} + \frac{P_{HL}}{I_A}, \tag{21}$$

giving the total power consumption in watts per ampere. This expression is similar to (18), again indicating the mercury pool arc to be more efficient because of less power lost in heat radiation and heat conduction at the cathode.

Thus, it may be said that from the point of view of the over-all power consumption, the low boiling point metal arc can operate more efficiently than any other known arc type. Since it is most likely that an arc will establish itself in the most energetically favorable mode of operation it must be assumed that wherever a thermionic arc exists the formation of a non-thermionic arc is either prohibited or conditions for its maintenance non-existing. Such a necessary condition for the maintenance of a non-thermionic type of arc might be the existence of a high vapor pressure adjacent to the cathode surface. Engel and Steenbeck[15] formulate this requirement in the following way: whether a non-thermionic or thermionic arc establishes itself seems to depend on whether, when heating the cathode, evaporation of cathode material or thermionic emission sets in first.

Karl G. Hernqvist

REFERENCES

1. K. G. Hernqvist and E. O. Johnson, *Phys. Rev.* 98, 1576 (1955).
2. E. O. Johnson, *RCA Rev.* 16, 498 (1955).
3. J. Kömmick, *Ann. D. Physik.* 12, 273 (1932).
4. S. Wagener, THE OXIDE-COATED CATHODE, Vol. 2, pp. 78-79, Chapman and Hall Ltd., London (1951).
5. M. J. Druyvesteyn and F. M. Penning, *Rev. Mod. Phys.* 12, 87 (1940).
6. C. G. Smith, *Phys. Rev.* 69, 96 (1946).
7. G. Steer, *Zeitschr. f. angew. Physik,* 5, 116 (1953).
8. D. Zei, R. St. John and J. G. Winans, *Phys. Rev.,* 100, 1232 (1955).
9. R. M. St. John and J. G. Winans, *Phys. Rev.* 98, 1664 (1955).
10. C. J. Gallagher, *J. Appl. Phys.* 21, 768 (1950).
11. M. Knoll, F. Ollendorff, and R. Rompe, GASENTLADUNGSTABELLEN, p. 50, Springer Verlag, Berlin (1935).
12. A. v. Engel and M. Steenbeck, ELEKTRISCHE GASENTLADUGEN, vol. 2, p. 86, Table 2, Springer Verlag, Berlin (1934). A value of a constant c is given for mercury, from which can be computed the ion mobility $\mu^+ = 219$ cm^2/voltcm, ion diffusion constant $D^+ = 5$ cm^2/sec and electron mobility $\mu^- = 5.2 \times 10^5$ cm^2/voltsec, all at a pressure of 1 mm of mercury and a temperature of 273°K.
13. G. Mierdel, *Zeitschr f. tech. Physik* 17, 452 (1936).
14. O. Engelbrecht, *Archiv f. Electrotechnik* 36, 515 (1942).
15. A. v. Engel and M. Steenbeck ELEKTRISCHE GASENTALADUNGEN, Vol. 2, pp. 119-138, Springer Verlag, Berlin (1934).
16. E. W. Müller, *Zeitschr. f. Physik* 120, 261 (1943).
17. W. S. Boyle, P. Kisliuk, and L. H. Germer, *J. Appl. Phys.*, 26, 720 (1955).
18. J. Rothstein, *Phys. Rev.* 73, 1214 (1948).
19. K. D. Froome, *Proc. Phys. Soc.* 62B, 805 (1949).
20. S. S. Mackeown, *Phys. Rev.* 34, 611 (1929).
21. T. Wasserrab, *Zeitschr. f. Physik* 130, 311 (1951).
22. R. Rompe and M. Steenbeck, *Erg. d. exakt. Naturwiss.* 18, 257 (1939).
23. L. Malter, E. O. Johnson, and W. M. Webster, *RCA Rev.* 12, 415 (1951).